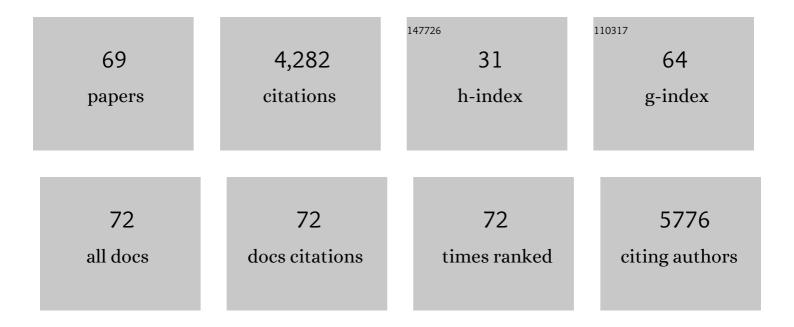
Willie J C Geerts

List of Publications by Year in descending order

Source: https://exaly.com/author-pdf/4564689/publications.pdf Version: 2024-02-01



#	Article	IF	CITATIONS
1	Cellular Metabolism Regulates Contact Sites between Vacuoles and Mitochondria. Developmental Cell, 2014, 30, 86-94.	3.1	285
2	Secretory traffic triggers the formation of tubular continuities across Golgi sub-compartments. Nature Cell Biology, 2004, 6, 1071-1081.	4.6	283
3	ER-to-Golgi Carriers Arise through Direct En Bloc Protrusion and Multistage Maturation of Specialized ER Exit Domains. Developmental Cell, 2003, 5, 583-594.	3.1	225
4	Correlative microscopy and electron tomography of GFP through photooxidation. Nature Methods, 2005, 2, 857-862.	9.0	207
5	Atg9 establishes Atg2-dependent contact sites between the endoplasmic reticulum and phagophores. Journal of Cell Biology, 2018, 217, 2743-2763.	2.3	194
6	Small cargo proteins and large aggregates can traverse the Golgi by a common mechanism without leaving the lumen of cisternae. Journal of Cell Biology, 2001, 155, 1225-1238.	2.3	185
7	Combined structural and chemical analysis of the anammoxosome: A membrane-bounded intracytoplasmic compartment in anammox bacteria. Journal of Structural Biology, 2008, 161, 401-410.	1.3	176
8	Immuno-electron tomography of ER exit sites reveals the existence of free COPII-coated transport carriers. Nature Cell Biology, 2006, 8, 377-383.	4.6	173
9	Linking Ultrastructure and Function in Four Genera of Anaerobic Ammonium-Oxidizing Bacteria: Cell Plan, Glycogen Storage, and Localization of Cytochrome <i>c</i> Proteins. Journal of Bacteriology, 2008, 190, 708-717.	1.0	163
10	The platelet interior revisited: electron tomography reveals tubular α-granule subtypes. Blood, 2010, 116, 1147-1156.	0.6	156
11	EGFR Dynamics Change during Activation in Native Membranes as Revealed by NMR. Cell, 2016, 167, 1241-1251.e11.	13.5	153
12	AP-1 and KIF13A coordinate endosomal sorting and positioning during melanosome biogenesis. Journal of Cell Biology, 2009, 187, 247-264.	2.3	146
13	SNX1 Defines an Early Endosomal Recycling Exit for Sortilin and Mannose 6â€Phosphate Receptors. Traffic, 2008, 9, 380-393.	1.3	145
14	Electron tomography of early melanosomes: Implications for melanogenesis and the generation of fibrillar amyloid sheets. Proceedings of the National Academy of Sciences of the United States of America, 2008, 105, 19726-19731.	3.3	133
15	Biogenesis of the demarcation membrane system (DMS) in megakaryocytes. Blood, 2014, 123, 921-930.	0.6	112
16	Contribution of high-resolution correlative imaging techniques in the study of the liver sieve in three-dimensions. Microscopy Research and Technique, 2007, 70, 230-242.	1.2	97
17	Colgi Enzymes Are Enriched in Perforated Zones of Golgi Cisternae but Are Depleted in COPI Vesicles. Molecular Biology of the Cell, 2004, 15, 4710-4724.	0.9	90
18	Complementary distribution of carbamoylphosphate synthetase (ammonia) and glutamine synthetase in rat liver acinus is regulated at a pretranslational level Journal of Histochemistry and Cytochemistry, 1988, 36, 751-755.	1.3	86

WILLIE J C GEERTS

#	Article	IF	CITATIONS
19	Automated high-throughput electron tomography by pre-calibration of image shifts. Journal of Microscopy, 2002, 205, 187-200.	0.8	84
20	An evidence based hypothesis on the existence of two pathways of mitochondrial crista formation. ELife, 2016, 5, .	2.8	81
21	STEM tomography in cell biology. Journal of Structural Biology, 2007, 159, 381-391.	1.3	71
22	lsomyosin expression pattern during formation of the tubular chicken heart: A three-dimensional immunohistochemical analysis. The Anatomical Record, 1990, 226, 213-227.	2.3	59
23	Ultrastructure of the Denitrifying Methanotroph "Candidatus Methylomirabilis oxyfera,―a Novel Polygon-Shaped Bacterium. Journal of Bacteriology, 2012, 194, 284-291.	1.0	56
24	Membrane Contact Sites between Apicoplast and ER in <i>Toxoplasma gondii</i> Revealed by Electron Tomography. Traffic, 2009, 10, 1471-1480.	1.3	55
25	Cell division ring, a new cell division protein and vertical inheritance of a bacterial organelle in anammox planctomycetes. Molecular Microbiology, 2009, 73, 1009-1019.	1.2	53
26	Mast Cell Degranulation Is Accompanied by the Release of a Selective Subset of Extracellular Vesicles That Contain Mast Cell–Specific Proteases. Journal of Immunology, 2016, 197, 3382-3392.	0.4	49
27	High protein diet induces pericentral glutamate dehydrogenase and ornithine aminotransferase to provide sufficient glutamate for pericentral detoxification of ammonia in rat liver lobules. Histochemistry and Cell Biology, 1999, 111, 445-452.	0.8	47
28	Template matching as a tool for annotation of tomograms of stained biological structures. Journal of Structural Biology, 2007, 158, 327-335.	1.3	41
29	The local expression of adult chicken heart myosins during development. Anatomy and Embryology, 1986, 174, 187-193.	1.5	40
30	Basic strategies for valid cytometry using image analysis. The Histochemical Journal, 1997, 29, 347-364.	0.6	39
31	Threeâ€dimensional organization of fenestrae labyrinths in liver sinusoidal endothelial cells. Liver International, 2009, 29, 603-613.	1.9	39
32	TRIM46 Organizes Microtubule Fasciculation in the Axon Initial Segment. Journal of Neuroscience, 2019, 39, 4864-4873.	1.7	38
33	Endosome-mediated autophagy. Autophagy, 2013, 9, 861-880.	4.3	35
34	Image analysis and image processing as tools to measure initial rates of enzyme reactions in sections: distribution patterns of glutamate dehydrogenase activity in rat liver lobules Journal of Histochemistry and Cytochemistry, 1995, 43, 1027-1034.	1.3	31
35	3-D Structure of Multilaminar Lysosomes in Antigen Presenting Cells Reveals Trapping of MHC II on the Internal Membranes. Traffic, 2004, 5, 936-945.	1.3	28
36	New comprehension of the apicoplast of Sarcocystis by transmission electron tomography. Biology of the Cell, 2006, 98, 535-545.	0.7	28

WILLIE J C GEERTS

#	Article	IF	CITATIONS
37	Synovial fluid pretreatment with hyaluronidase facilitates isolation of CD44+ extracellular vesicles. Journal of Extracellular Vesicles, 2016, 5, 31751.	5.5	28
38	Arginine π-stacking drives binding to fibrils of the Alzheimer protein Tau. Nature Communications, 2020, 11, 571.	5.8	28
39	Distribution pattern of acetylcholinesterase in early embryonic chicken hearts. The Anatomical Record, 1990, 228, 297-305.	2.3	19
40	Gender-dependent regulation of glutamate dehydrogenase expression in periportal and pericentral zones of rat liver lobules Journal of Histochemistry and Cytochemistry, 1996, 44, 1153-1159.	1.3	19
41	Trans-Membrane Area Asymmetry Controls the Shape of Cellular Organelles. International Journal of Molecular Sciences, 2015, 16, 5299-5333.	1.8	19
42	cDNA sequence of the long mRNA for human glutamine synthase. Biochimica Et Biophysica Acta Gene Regulatory Mechanisms, 1991, 1090, 249-251.	2.4	18
43	Quantitative graphical description of portocentral gradients in hepatic gene expression by image analysis. Hepatology, 1997, 26, 398-406.	3.6	17
44	The v-Crk Oncogene Enhances Cell Survival and Induces Activation of Protein Kinase B/Akt. Journal of Biological Chemistry, 2001, 276, 25176-25183.	1.6	17
45	A vaccinia virus lacking A10L: viral core proteins accumulate on structures derived from the endoplasmic reticulum. Cellular Microbiology, 2006, 8, 427-437.	1.1	17
46	Cobblestone HUVECs: A human model system for studying primary ciliogenesis. Journal of Structural Biology, 2011, 176, 350-359.	1.3	17
47	Immuno―and Correlative Light Microscopyâ€Electron Tomography Methods for <scp>3D</scp> Protein Localization in Yeast. Traffic, 2014, 15, 1164-1178.	1.3	17
48	Spatial organization of the transforming MHC class II compartment. Biology of the Cell, 2010, 102, 581-591.	0.7	16
49	Creatine kinase isozyme expression in embryonic chicken heart. Anatomy and Embryology, 1989, 179, 387-393.	1.5	14
50	Correction of autofocusing errors due to specimen tilt for automated electron tomography. Journal of Microscopy, 2003, 211, 179-185.	0.8	14
51	MRI monitoring of nanocarrier accumulation and release using Gadoliniumâ€SPIO coâ€labelled thermosensitive liposomes. Contrast Media and Molecular Imaging, 2016, 11, 184-194.	0.4	14
52	Hyperthermia-triggered release of hypoxic cell radiosensitizers from temperature-sensitive liposomes improves radiotherapy efficacy <i>in vitro</i> . Nanotechnology, 2019, 30, 264001.	1.3	14
53	In Situ Measurement of Glutamate Concentrations in the Periportal, Intermediate, and Pericentral Zones of Rat Liver. Journal of Histochemistry and Cytochemistry, 1997, 45, 1217-1229.	1.3	13
54	Zinc binding regulates amyloid-like aggregation of GAPR-1. Bioscience Reports, 2019, 39, .	1.1	13

WILLIE J C GEERTS

#	Article	IF	CITATIONS
55	Lobular patterns of expression and enzyme activities of glutamine synthase, carbamoylphosphate synthase and glutamate dehydrogenase during postnatal development of the porcine liver. Biochimica Et Biophysica Acta - General Subjects, 1994, 1200, 265-270.	1.1	12
56	Shortening of membrane lipid acyl chains compensates for phosphatidylcholine deficiency in cholineâ€auxotroph yeast. EMBO Journal, 2021, 40, e107966.	3.5	12
57	The dynamics of local kinetic parameters of glutamate dehydrogenase in rat liver. Histochemistry and Cell Biology, 1996, 106, 437-443.	0.8	9
58	Marked mitochondrial alterations upon starvation without cell death, caspases or Bcl-2 family members. Biochimica Et Biophysica Acta - Molecular Cell Research, 2008, 1783, 2013-2019.	1.9	9
59	Foreword to the themed issue on correlative microscopy. Journal of Microscopy, 2009, 235, 239-240.	0.8	7
60	Immunohistochemical analysis of the distribution of histone H5 and hemoglobin during chicken development. Differentiation, 1987, 34, 161-167.	1.0	6
61	Electron Tomography and Correlative Approaches in Platelet Studies. Methods in Molecular Biology, 2018, 1812, 55-79.	0.4	5
62	The dynamics of local kinetic parameters of glutamate dehydrogenase in rat liver. Histochemistry and Cell Biology, 1996, 106, 437-443.	0.8	5
63	A Novel Method of Data Collection for Automated Electron Tomography Based upon Pre-cal1bration of Image Shifts and Defocus Changes. Microscopy and Microanalysis, 2001, 7, 78-79.	0.2	3
64	Differences in erythropoiesis in normal chicken and quail embryos. The Histochemical Journal, 1993, 25, 280-290.	0.6	2
65	D-CAT: Density and Clustering Annotation Tool for three dimensional electron microscopic volumes. Journal of Structural Biology, 2012, 177, 571-577.	1.3	1
66	Computer-Controlled Transmission Electron Microscopy: Automated Tomography. Microscopy and Microanalysis, 2001, 7, 968-969.	0.2	0
67	TEM and STEM Tomography for the Detection of Ultra Small Gold Labels within Stained and Plastic-Embedded Sections of Tissue. Microscopy and Microanalysis, 2003, 9, 1172-1173.	0.2	0
68	Hepatic steatosis and congenital portosystemic shunts: a threeâ€dimensional transmission electron microscopic view. Liver International, 2009, 29, 884-885.	1.9	0
69	Combined structural and chemical analysis of unique anammox bacteria that contain a prokaryotic organelle. , 2008, , 65-66.		0